Noise suppression and multiple attenuation using full-azimuth angle domain imaging: case studies

Aleksander Inozemtsev[1*], Zvi Koren[1] and Alexander Galkin[2] propose a method to minimize the effort to condition/clean the recorded data during the processing stage.

The EarthStudy 360 Imager is an advanced depth imaging system that first maps the full recorded seismic data into the subsurface grid points and then decomposes the data into local angle domain (LAD) bins. It is based on specially designed diffraction operators using bottom-up ray tracing. In this article, we focus on the ability of the EarthStudy 360 Imager to attenuate different types of wave characteristics considered as both random and coherent noise – in particular, different orders of multiples, and non-reflection seismic events such as Rayleigh, refraction, diffraction and 'side' waves. The method is based on internal implementation of local slant stack (LSS) operators optimally designed for each primary ray pair associated with a given source-image point-receiver path and the corresponding seismic data event. The LSS is applied in the direction of the horizontal slowness components of the arriving rays at the acquisition surface, where the size of the LSS (the number of traces involved) is computed independently for each ray pair from its first Fresnel zone. Thus, primary reflection events sharing the same traveltime and the same surface directivity as the traced ray pairs are emphasized (highly weighted), while all other events (considered as noise) are simultaneously attenuated. We demonstrate our method in four different land data examples with different levels of geological complexities.

Noise suppression and multiple attenuation are the most time-consuming and still the most challenging tasks in seismic processing, to condition seismic data for velocity analysis, imaging and amplitude inversions. This type of operation requires special expertise to set up specific workflows of dedicated technologies to be run on massive parallel computation systems. Nevertheless, even when using the most advanced methods, some signatures of the noisy components and the different orders of multiples remain within the processed data. Moreover, any attempt to attenuate these 'artifacts' results in also attenuating actual primary reflecting events.

In this paper, we suggest minimizing the effort to condition/clean the recorded data during the processing stage, since noise suppression and multiple attenuation are naturally performed within the imaging stage. The method is based on a US patent (Koren, 2006) and further explained in the paper by Koren and Ravve (2011). The method is implemented using a special imaging technique, referred to as EarthStudy 360 Imager, in which the full recorded dataset is first mapped into the subsurface grid points and then decomposed into four-dimensional local angle domain bins at each point. The mapping and the binning are performed using special bottom-up diffraction ray tracing where each seismic event associated with a given image point is related to a given primary ray pair consists of a 'source ray' and a corresponding 'receiver ray'. The method is oriented to enhance primary events and simultaneously attenuate all other types of seismic events. It is based on the internal implementation of local slant stack (LSS) operators optimally designed for each primary of the ray pairs. The LSS is applied in the direction of the horizontal slowness components of the arriving rays at the acquisition surface, where the size of the LSS (the number of traces involved) is computed independently for each ray pair from its first Fresnel zone. Thus, primary reflection events sharing the same traveltime and the same surface directivity as the traced ray pairs are emphasized (highly weighted) while all other events (considered as noise) are simultaneously attenuated. The ability of the method to suppress noisy characteristics within the data, and in particular to attenuate different types of multiples, is demonstrated in four different land data examples with different levels of geological complexity.

Method: Local slant stacks and beam steering

The proposed method is directly related to beam-type migrations, where our unique implementation provides optimal ways to ensure that primary seismic events will be highlighted (enhanced) by the migration operator and all other types of seismic characteristics, considered here as 'noise', will be simultaneously attenuated.

[1] *Paradigm.*
[2] *Zapprikaspiygeofizika.*
[*] *Corresponding author, E-mail: Alexander.Inozemtsev@PDGM.com*

Gaussian Beam migrations (e.g., Hill, 2001; Gray and Bleistein, 2009; Gray et al., 2009) have been successfully implemented in improving Kirchhoff-based migrations in complex geological areas, especially where the wavefield includes multi-pathing. Fast beam steering migrations (e.g., Sherwood et al., 2009) have also become very popular, especially for velocity model building where only the energetic beams are stored and used. These beam migrations require preprocessing of the recorded seismic data traces prior to the migration. The construction of beams is based on a local tapered slant stack approach, which is normally performed for a coarse grid, depending on the dominant frequency of the input data. The local slant stack approach normally enhances signal-to-noise ratio, and therefore improves continuity of the structural image. Note that every beam event is associated with traveltime, shot-receiver areas and directivity. In our beam implementation, however, the beams are performed on-the-fly throughout the decomposition/imaging stage, where for each ray pair, a set of proximity sources around the 'source ray' and the corresponding receivers at the vicinity of the 'receiver ray' are collected to form the slant stack process. The proximity for each ray is individually computed with the estimated local Fresnel zone. The Fresnel zones are assumed to be elliptic projections of circular regions around the central source ray and the central receiver ray on the earth's surface, with major semi-axes $R_F^{\mathrm{maj}}(M,S)$ and $R_F^{\mathrm{maj}}(M,R)$, respectively,

$$R_F^{\mathrm{maj}}(\mathbf{M},\mathbf{S})=\sqrt{\frac{|J(\mathbf{M},\mathbf{S})|}{f_D}},\ R_F^{\mathrm{maj}}(\mathbf{M},\mathbf{R})=\sqrt{\frac{|J(\mathbf{M},\mathbf{R})|}{f_D}}. \quad (1)$$

For each ray ('source' and 'receiver'), the ratio between the minor and major semi-axes depends on the dip angle ν_1^{surf} of the phase velocity at the earth surface point, $R_F^{\mathrm{min}}/R_F^{\mathrm{maj}}=\cos\nu_1^{\mathrm{surf}}$, and the eccentricity of the elliptic zone is $\xi_F=\sin\nu_1^{\mathrm{surf}}$. In case of a tilted topographic surface, we replace the dip angle ν_1^{surf} with the angle between the phase velocity and the normal to the topography. Thus, the area of the proximity $A_F=\pi R_F^{\mathrm{min}}R_F^{\mathrm{maj}}$ is estimated from the ray Jacobian J of each individual ray and the dominant frequency f_D of the recorded data. The slant (slope) used for the local stack is taken from the slowness vectors of the 'source ray' $\mathbf{p}^S$ and the 'receiver ray' $\mathbf{p}^R$, respectively. The local tapered slant stack event can be constructed by

$$U_{\mathrm{beam}}(\mathbf{S}_o,\mathbf{R}_o,t)=\frac{1}{N_f}\iint_{\partial S\,\partial R}U(\mathbf{S}_o+\Delta\mathbf{S},\mathbf{R}_o+\Delta\mathbf{R},t+\Delta\tau)\,f_{\mathrm{taper}}(\Delta\mathbf{S},\Delta\mathbf{R})\,d\mathbf{S}\,d\mathbf{R} \quad (2)$$

where N_f is a normalization factor, $\Delta\mathbf{S}=\{\Delta x_S,\Delta y_S,\Delta z_S\}$, $\Delta\mathbf{R}=\{\Delta x_R,\Delta y_R,\Delta z_R\}$ are the shifts between central and 'current' locations of sources/receivers of the stacked traces within the local areas bounded by the Fresnel zones, along the acquisition surface $z = z\,(x,\,y)$. Function $U(\mathbf{S}_o+\Delta\mathbf{S},\mathbf{R}_o+\Delta\mathbf{R},t+\Delta\tau)$ is the recorded seismic data, $t=t(\mathbf{M},\mathbf{S}_o,\mathbf{R}_o)$ is the two-way traveltime of the central rays, $f_{\mathrm{taper}}(\Delta\mathbf{S},\Delta\mathbf{R})$ is a Gaussian taper, and $\Delta\tau$ is the traveltime correction due to the above-mentioned shifts,

$$\begin{aligned}\Delta\tau&=\Delta\tau_S+\Delta\tau_R\\&=p_x^S\Delta x_S+p_y^S\Delta y_S+p_z^S\Delta z_S+p_x^R\Delta x_R+p_y^R\Delta y_R+p_z^R\Delta z_R.\end{aligned} \quad (3)$$

Thus, the construction of the local beams to be migrated for each point and each ray pair is theoretically more accurate than the standard beam migrations, where the beam construction is uniformly performed prior to the migration. A beam steering approach can then be applied by measuring the coherency (e.g., semblance) of the candidate wavelets before the performance of the slant stack, where only energetic events are migrated.

Field examples

Western Siberia

The recorded seismic data in this area is characterized by a large number of different order high-amplitude multiples. The multiple events are generated from different depth interfaces between various rock types, starting from the Upper Cretaceous clastic sediments at the shallow-medium parts of the subsurface and going deeper. 'Trains' of multiple waves are amplified in the range of low-amplitude reflections from the Neocomian Terrigenous strata (layers marking BC), including the wedge Achimov sediments, which are concentrated in sand and siltstone reservoirs of oil and gas. Multiple reflections of different orders are superimposed on the high-contrast reflections scattered from the clastic sediments of the Jurassic formations, in which the oil-bearing strata are often deposits J0, J2-J3.

Figure 1 shows a comparison between depth images and common image gathers (CIG) generated by Kirchhoff PSDM (left) and the EarthStudy 360 Imager (right), where the same input data, migration aperture, frequency band and velocity model were used. Unlike the result from the Kirchhoff PSDM, it is clearly shown that the EarthStudy 360 Imager managed to almost completely attenuate the different types of multiples over the entire depth range (H2-Pz). The migrated full-azimuth reflection events are continuous and balanced across the entire range of reflection angles. Deeper migrated events begin to show subtle effects of ruffling or quasi-sinusoidal occurrence associated with changes in the stress state of rocks and the presence of fractured zones. Note that this quasi-sinusoidal form is the way migrated seismic events manifest azimuthal anisotropy, such as orthorhombic or HTI layers.

The vertical semblance plot along the full-azimuth reflection angle gather (Figure 1B) shows clear, high-resolution, zero RMO coherency along the entire depth range, whereas in the Kirchhoff PSDM, the semblance plot is very noisy due to the existence of multiples.

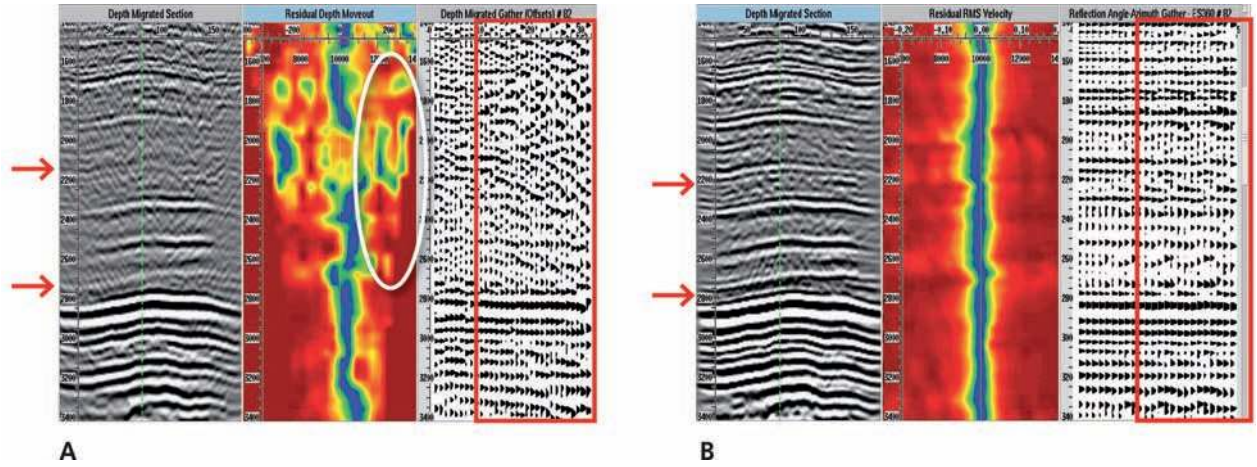

Figure 1 *Comparison of the results of attenuating multiples in the full-azimuth depth migration at the level of gathers, images and residual spectrum. A: (left to right): Depth image, residual moveout semblance and 3D depth offset gather (OVT) after Kirchhoff PSDM. B: Depth image, residual moveout semblance and 3D depth full-azimuth angle gather after EarthStudy 360 imager in the mode of multiples suppression (LSS – operator's filtering).*

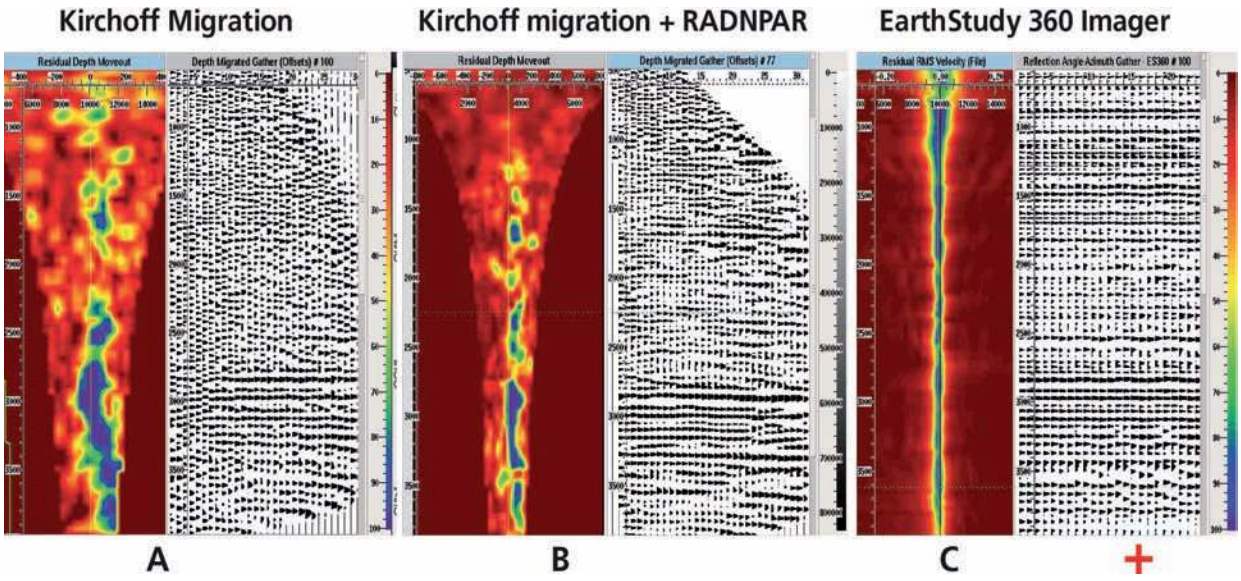

Figure 2 *A comparison of the attenuation of multiple reflections. Figure 2A shows the Kirchhoff PSDM offset gather and the corresponding noisy semblance profile. Figure 2B shows the partial improvement obtained when applying parabolic Radon multiple attenuation on this gather. Figure 3C demonstrates the power of the LSS operator within the EarthStudy 360 Imager.*

Figure 2 compares the results of the attenuation of multiple reflections which completely mask the real reflecting boundaries, in particular at the Neocomian strata and Upper Cretaceous deposits. Figure 2A shows the Kirchhoff PSDM offset gather and the corresponding noisy semblance profile. Figure 2B shows the partial improvement obtained when applying parabolic Radon multiple attenuation to this gather. Figure 3C shows the power of the LSS operator within the EarthStudy 360 Imager, where all 'train' high-amplitude multiples are attenuated and the primary reflection events, including the subtle azimuthally variation in the Achimov Formation and the Jurassic, are significantly highlighted.

Figure 3 focuses on multiples attenuation along the Jurassic and Paleozoic basement. Again, using the Kirchhoff PSDM (Figure 3A), the shape of the low amplitude migrated reflectivities are distorted by these types of inter-bed multiples. A multiple reflection event crossing the whole lateral range strongly dominates this area, forming a complex image that can barely be interpreted. On the other hand, the EarthStudy 360 Imager (Figure 3B) provides a clearer and more realistic image of the complex geological structure of the Paleozoic basement. Additionally, a system of subvertical faults and clear boundaries between the Jurassic and Paleozoic basement is noted. The sinusoidal azimuthal characteristic of this reflected event along the full-azimuth image gather indicates the existence of azimuthal anisotropic layers, mainly manifested with the aligned system of vertical faults.

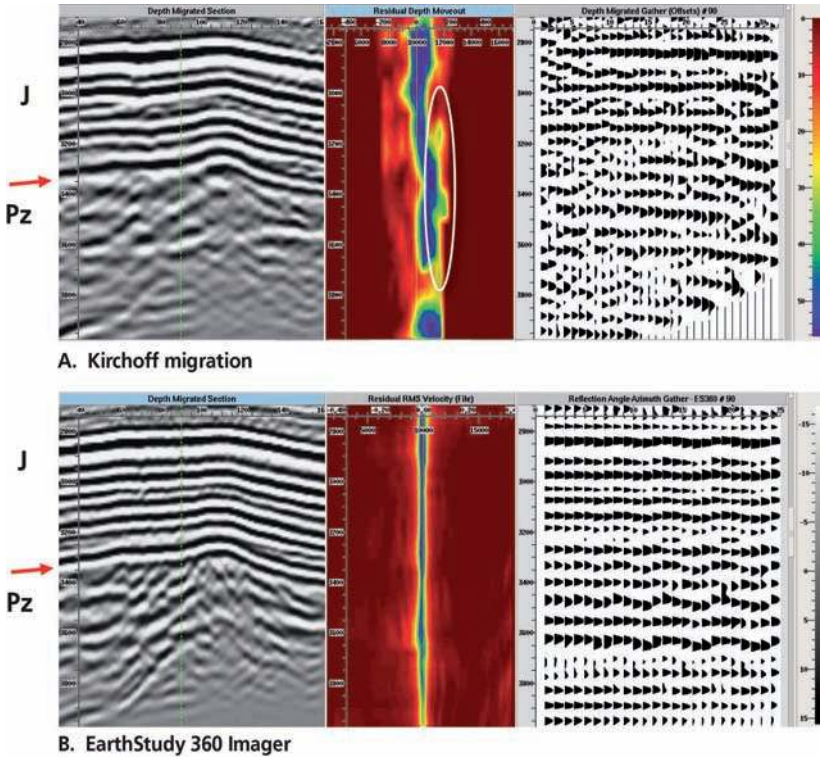

Figure 3 *Comparison of multiples attenuation along the Jurassic and Paleozoic basement. Figure 3A shows the Kirchhoff PSDM result, where Figure 3B shows The EarthStudy 360 Imager which provides a cleaner and more realistic image of the complex structure of the Paleozoic basement.*

Eastern Siberia

The Eastern Siberia region contains shallow sedimentary layers with the frequent appearance of thin beds of different lithologies characterized by high velocities. From top to bottom, these layers can be classified with the following types of rocks: Trappean, igneous rocks, salt formations, clay, fractured carbonate and sediments of dolomite, clastic shale strata, and carbonate sediments followed by igneous and complex metamorphic rocks of the Riphean basement. In this area, oil-saturated reservoirs are confined as carbonate and clastic strata, complex Vendian rocks and weathering crust Riphean basement. The alternation of the contrasting boundaries forms a dense low-power field of multiple waves with moveout similar to the moveout of primary reflections (Figure 4A). Additionally, contrasting boundaries of igneous basalt form regular high-amplitude refracted waves, which also complicate tracking of primary waves at large distances. Standard noise suppression programmes (Figure 4B) only partially solve the problem of tracking primary reflections. The LSS operator within the EarthStudy 360 Imager managed to provide clean, vertical high-resolution angle gathers, free of multiples (Figure 4C).

Middle Volga

The geological section of the sedimentary rocks of the Middle Volga is similar to that of Eastern Siberia, with thicker sedimentary rocks of different lithology and age. However, the presence of clay, sandstone, dolomite and salt formations creates strong contrasts in the main reflectors and generates favorable conditions for the emergence of a massive 'train' of multiple waves of different orders. In many cases, this effect is so strong that none of the traditional multiple attenuation programmes can provide a sufficient solution for suppressing these inter-bed strong multiples (Figure 5A). For these reasons, under these conditions, multiple suppression is often simply not used.

Figure 5B again shows the ability of the EarthStudy 360 Imager with its LSS operator to considerably attenuate the high-amplitude inter-bed multiples, especially critical across the carbonate strata that include the target oil-bearing reefs. The effect of the aligned near-vertical fractures within the carbonate layers is clearly seen along the full-azimuth angle gathers with the azimuthally periodicity of the main reflectors. In this case, the fracture density and intensity are larger than in the case of clastic rocks, where the sinusoidal form is therefore more dominant. The depth image is sharper, containing higher-resolution geological features. The corresponding vertical semblance profiles are much clearer, with noticeable coherency.

Figure 6 further shows the noise/multiples attenuated image and image gather, generated by the EarthStudy 360 Imager, along the entire geological section (up to 5 km in depth). The clean results are manifested from the upper sandstone and carbonate formation, through the salt sheets, down to the Terigenna and Upper Devonian strata. Note that the subtle effects of azimuthal anisotropy, which are absent in the upper part of the section, sharply increase in intensity when entering the complex carbonate area

(H = 2500-3700 m) and then fall sharply in the Devonian Terrigenous clayed strata (H = 3700-4400 m).

Salt Dome Tectonics

This paper presents another comparison between a Kirchhoff PSDM and the EarthStudy 360 migration, for imaging along and below complex geological areas containing salt domes. The high-velocity contrasts between the surrounding sediments and the salt bodies, the rough transition zones, and especially the steep salt flanks, make imaging in such areas extremely challenging. Inter-salt multiples and other types of multiples mask the principal primary reflectivities.

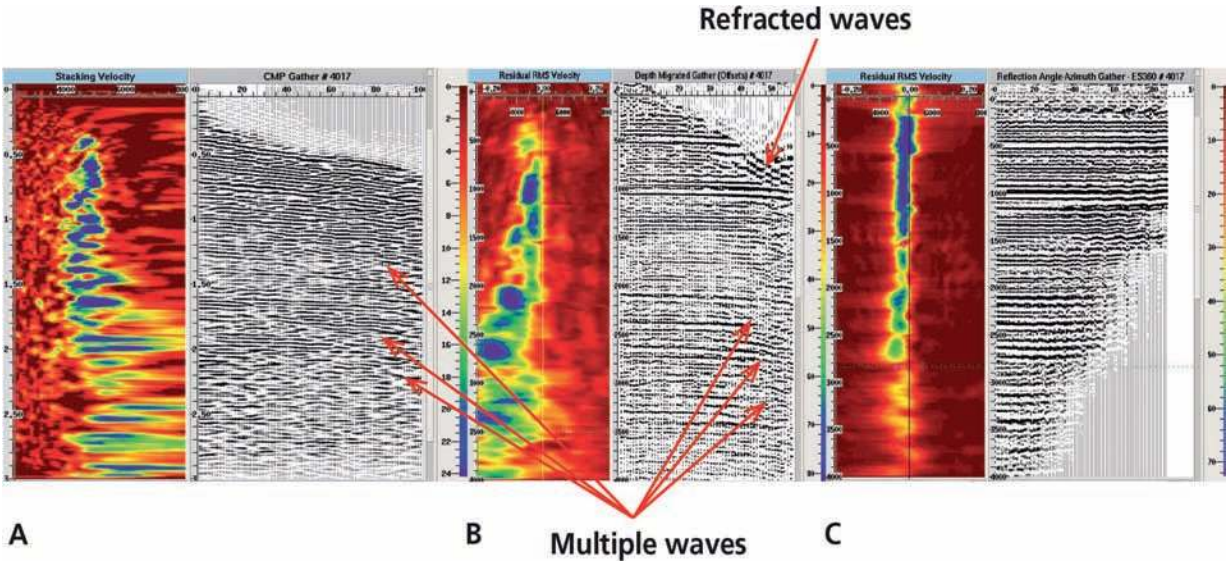

Figure 4 *Figure 4A shows the result of common offset gather generated by Kirchhoff PSDM with the corresponding chaotic semblance profile. Figure 4B shows the same gather after after the Kirchhoff migration and the application of random noise suppression and Radon-based multiples attenuation, where the RMO semblance profile is much improved. Figure 4C again shows considerable improvement due to the application of the LSS operator in the EarthStudy 360 Imager. The high-resolution vertical semblance indicates the high level of continuity in the angle domain reflected events.*

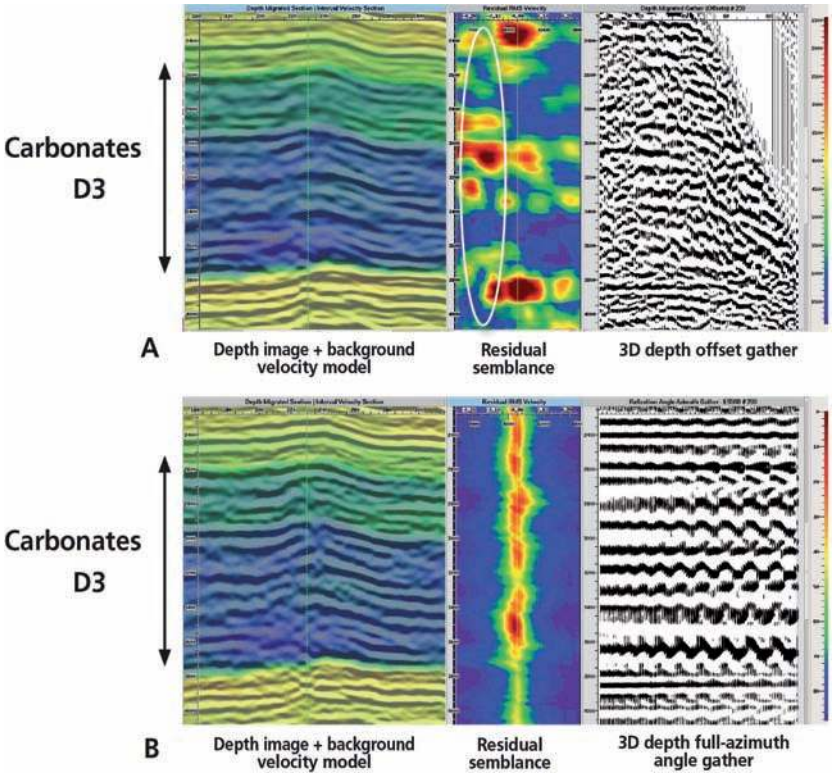

Figure 5 *A comparison of the depth image, spectrum residual velocity and migrated gathers. A- after Kirchhoff migration, B - after EarthStudy 360 migration using an LSS operator to suppress multiple waves of a different order. Carbonate reservoirs, Middle Volga.*

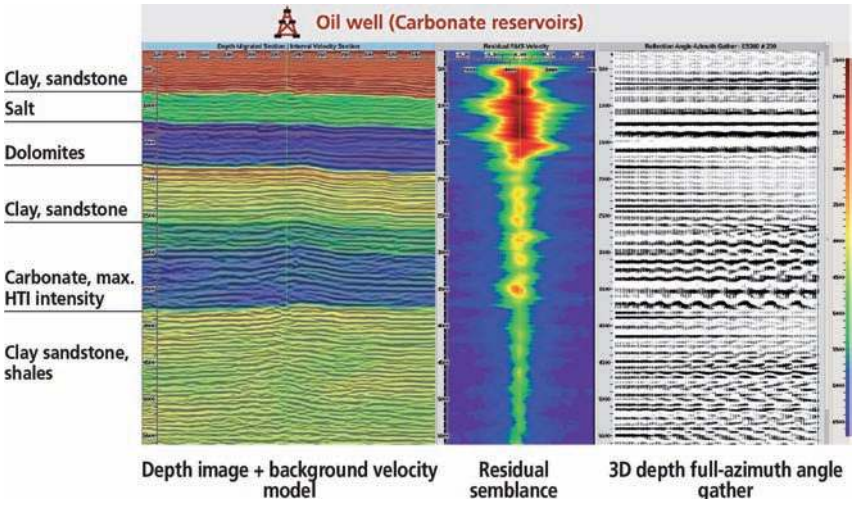

Figure 6 *High resolution clean of noise and multiples, depth image, and a selected full-azimuth angle gather in the Middle Volga survey.*

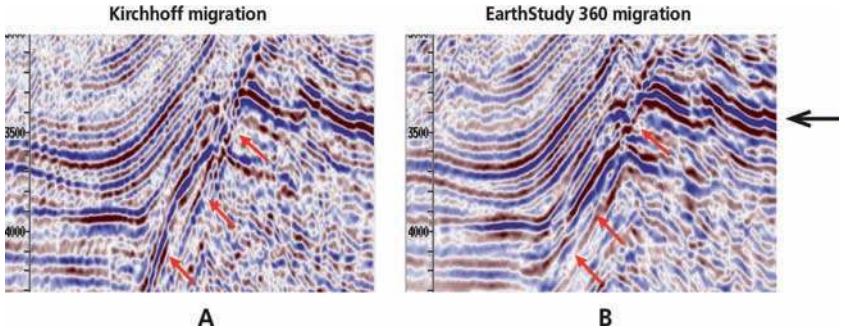

Figure 7 *Figure 7A shows the image obtained by Kirchhoff PSDM, where the transition zone along the salt flank is masked by 'side' waves and different types of multiples. Figure 7B shows the result of the EarthStudy 360 Imager with the LSS operator, providing a cleaner image and more geological plausible sub-structures (oil traps are marked by red arrows). The black arrow indicates the position of the main reservoir's stratum.*

'Side' waves reflecting, once and even more, from the steep salt flanks can be also considered noisy data, which are difficult to attenuate using conventional technology. It can be seen that the EarthStudy 360 Imager provides a cleaner and sharper image than the one generated by the Kirchhoff PSDM. The subtle structures in the transition zone between the steep sediments and the salt flanks are better defined, and the image is less affected by the interference of the inter-bed multiples.

Conclusion

In this paper, we have demonstrated an extremely powerful technique for noise suppression and multiples attenuation directly within the imaging stage, which minimizes the cumbersome and expensive processing operations which are regularly implemented to clean up and condition seismic gathers. The method is implemented using a special imaging system that maps the full recorded seismic data into the subsurface grid points and decomposes the data into the local angle domain bins. The internal suppression/attenuation of different types of noise and multiples is mainly achieved by optimally designing local slant stack (LSS) events (tapered local beams) which are highly weighted for the corresponding primary ray pairs traced throughout the subsurface velocity model, where all other types of seismic events are considered as 'noise' and therefore are naturally attenuated. The method is demonstrated in four representative land data examples, the last of which involves a dataset acquired over extremely complicated salt bodies.

Acknowledgment

The authors are grateful to the companies Syntez Pretroleum, Belorusneft and another anonymous one for their permission to show the results presented in this article.

References

Gray, S.H. and Bleistein, N. [2009] True-amplitude Gaussian-beam migration. *Geophysics*, **74** (2), S11-S23.

Gray, S.H., Xie, Y., Notfors, C., Zhu, T., Wang, D. and Ting, C.O. [2009] Taking apart beam migration. *The Leading Edge*, **28** (9), 1098-1108.

Hill, N.R. [2001] Prestack Gaussian-beam depth migration. *Geophysics*, **66** (4), 1240-1250.

Koren, Z. [2006] Multiple Suppression in Angle Domain Time and Depth Migration. United States (12) Patent Application Publication (10), Pub. No.: US 2006/0185929 A1 (Koren (43) Publication Date: 24 August, 2006).

Koren, Z. and Ravve, I. [2007] System and Method for Full-azimuth Angle Domain Imaging in Reduced Dimensional Coordinate Systems. Patent: US 20080109168 A1, 05/18/2007.

Koren, Z. and Ravve, I. [2011] Full-azimuth Subsurface Angle Domain Wavefield Decomposition and Imaging. *Geophysics*, 76 (1), P S1-S13.